

COVER PAGE

Document downloaded by @DAEL

Sat Nov 28 03:09:31 2026
For personal use

When automatic English translation is provided, only the original document is authentic.
The EAA cannot be held responsible of any translation error

Bibliographical reference

Dynamic Simulation of Traffic Noise by Applying Ray Tracing Method based on Indoor Space Partitioning, Zhibin Chen, Ming Cai, Feng Li and Weijia Ye, Acta Acustica **vol. 100** (Number 3), 2014, pp. 467-476

DOI
https://doi.org/10.3813/AAA.918727

ACTA ACUSTICA UNITED WITH ACUSTICA
Vol. 100 (2014) 467 – 476
DOI 10.3813/AAA.918727

Dynamic Simulation of Traffic Noise by Applying Ray Tracing Method based on Indoor Space Partitioning

Zhibin Chen[1)], Ming Cai[1)], Feng Li[2)], Weijia Ye[1)]
[1)] Research Center of Intelligent Transportation System, Sun Yat-sen University, Guangzhou 510275, China.
caiming@mail.sysu.edu.cn
[2)] Transportation Research Center of Zhongshan, Zhongshan 528400, China

Summary
This study presents a revised 3 dimensional ray tracing method by combining with indoor space partitioning. This method divides an entire indoor space into limited convex polyhedron subspaces, and thus reduces the number of surfaces intersected with rays, and omits the validity test of the collision point on the reflecting surfaces. Combining with a microscopic traffic simulation tool and a vehicle noise emission model, and taking the influence of diffraction into account, the method can be utilized inulating dynamically the process of traffic noise diffusing inside the building through windows. Meanwhile, this study selects two different types of architectural layouts in order to demonstrate this method's efficiency, the influence of diffraction and of the state of windows, the differences in indoor noise on different floors and the comparison of indoor and outdoor traffic noise distribution. A comparison study on before-and-after indoor space partitioning shows that the method is efficient, with about 60% optimization rate. Further, with windows open, the level difference between average indoor and outdoor traffic noise is 7.5 dB, while it can reach to 12.8 dB with windows closed.

PACS no. 43.50.Lj, 43.50.Rq

1. Introduction

Nowadays, traffic noise pollution is having a growingly negative impact on our daily work and life, with those who live and work in buildings near urban arterials suffering the most. Not only does traffic noise pollute the outdoor environment, it also influences the indoor acoustical environment through balconies and windows. Most recent researches of traffic noise pollution have focused on the overall situation in certain areas [1, 2, 3], such as residential, industrial and commercial areas, the sound field distribution of the exteriors and surroundings of buildings [4, 5, 6], the influence of traffic noise on different floors [7, 8], and the design of balconies [8, 9] and windows [10, 11]. However, little attention has been paid to the indoor sound field distribution [10]. The study of sound field distribution of indoor traffic noise has rarely been investigated as it is difficult to set up a sound field calculation analysis due to the mobility of sound sources and various ways of noise penetrating into indoor space (including diffraction, transmission). Nevertheless, an accurate sound field simulation and analysis of indoor traffic noise can provide the residents with advice on location and layout of buildings, from which property developers can use as a tool to reduce the indoor noise. Therefore, it is of great significance to simulate and analyze the indoor sound field caused by traffic noise.

With the development of traffic simulation technologies, dynamic traffic noise simulation has been more and more widely applied in the past few decades. Combining dynamic simulation of traffic flow with calculation of traffic noise, it can achieve dynamic simulation of traffic noise [12, 13, 14], which is of great accuracy and can reflect the dynamic variation of noise. At present, this method has been adopted in the prediction of traffic noise at signalized intersections [15, 16], crossings [17, 18, 19] and roundabouts [20]. However, the studies are mainly concentrated on the simulation of the outdoor environment. Rarely can we find research on dynamic simulation of indoor traffic noise.

Ray tracing is one of the popular methods to predict indoor sound fields with acceptable accuracy [21, 22]. It traces the transmission process of rays from sound source in all directions and can be applied in exploring dispersion [23], reflection and transmission of objects' surface [24]. It can also obtain accurate sound impulse response at the receiver [25, 26], and apply to the study of the reverberation in halls [27, 28, 29, 30]. However, when it comes to interconnected indoor space with multiple windows and doors, all the surfaces have to be traversed in order to get the collision point of the ray to the surface, and then the validity

Received 17 March 2013,
accepted 21 February 2014.

© S. Hirzel Verlag · EAA

of collision points has to be test. Thus, the whole process is complicated and cumbersome. Moreover, researches have been done to study the situation when the sound source is placed indoors [23, 28, 31, 32, 33], whereas the situation outdoors has been less covered.

In this paper, by combining ray tracing method with space partitioning, we propose an effective 3D ray tracing method applicable to different floors and arbitrary three-dimension indoor layouts. Incorporated with microscopic traffic simulation and considering the influence of diffraction, the proposed method can achieve a dynamic simulation of indoor traffic noise.

2. Methodology

2.1. Ray tracing method based on space partitioning

2.1.1. Classical 3D ray tracing method

The classical 3D ray tracing theory assumes that all surfaces in an enclosed space are flat, and the sound source transmits energy in the form of evenly sending out a large number of rays in every direction. Every single ray at the beginning carries the same amount of energy which is related to the number of sound rays. For any ray, the intersections of the ray and all the planes have to be calculated in order to find the perfect collision point of a certain ray to the surface, and the direction of the reflected ray is determined by the reflection law. Furthermore, the energy carried by the ray will be attenuated according to the reflection coefficient and the ray changes its moving routes every time it touches the surface. Until the energy of the ray gets lower than the pre-set threshold value, the computer will then stop tracing the ray and start following another. This process will be repeated until all the rays sent out by the source are marked. In this process, the arrival time and the amount of energy will be calculated and recorded once the ray passes through the receiver. Further, a series of sound pulses varying with time can be obtained by selecting a suitable time interval to count the sound energy at the receiver. Processing the sound pulses, the Sound Pressure Level (SPL) at the receiver can be obtained.

The general algorithm to determine the collision point of the ray to the surface includes two steps: firstly, find out all the intersections of the ray and all surfaces in the space; secondly, select the closest one from the starting point and examine whether it is effective (to make sure that the intersection is within the range of a real surface). If it is positive, it is the collision point; if not, again find the second closest one from the starting point and measure its effectiveness. This process will continue all the time until the unique collision point is found. If the target space is an enclosed convex polyhedron one, examining the effectiveness of the ray can be omitted since the closest intersection of the ray and surfaces will be undoubtedly located within the real surface. But if the space being studied is not an enclosed convex polyhedron space (such as semi-closed space with holes on the surface, concave polyhedron space, etc.), the effectiveness examination is necessary. Generally speaking, the intersection and surface need to be projected on a plane to further transform the 3D images into a question concerning the position relation between point and polygon in 2D space. Then Angle Summation Method, Cross product Method, Axis-Crossing Method and other methods [34, 35, 36] can be used to detect whether the collision point is valid or not, but these methods are so complex that they will definitely slow down the computation speed of ray tracing in practical 3D examples.

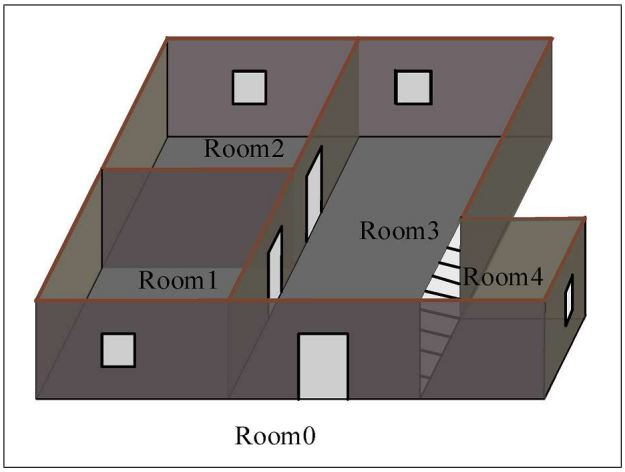

Figure 1. Schematic diagram of space division for indoor space.

2.1.2. The significance and rules of space partitioning

In order to skip the effectiveness examining of the intersections, reduce the number of surfaces which intersect with sound rays and improve the calculation efficiency, we propose a method of pre-processing using space partitioning, which divides a complex space into limited convex polyhedron subspaces defined as Rooms. Under general circumstance, we divide the indoor space into limited Rooms in accordance with the actual layout. For concave space, we add virtual doors (such as the shaded polygon in Figure 1) to divide it into two or more Rooms. Each Room connects to another through doors and windows after space partitioning (see Figure 1). Space partitioning has the following three characteristics: firstly, before the space partitioning starts the tracing, all the surfaces need to be traversed for the purpose of calculating the intersections, while only the surfaces confined in the Rooms need to be traversed with space partitioning. By this way, the searching range is narrowed down to a separate parts, hence a smaller number of surfaces are needed to find the intersections; secondly, an indoor space is not always a convex subspace before space partitioning, which renders the effectiveness examining essential. Due to the fact that the indoor space will be convex for sure after space partitioning, and the closest intersection must fall on a real surface, thus the effectiveness examining can be omitted; thirdly, after space partitioning the receivers are classified according to the Rooms they belong to, and only the ones in the Room where the ray is tracing should be traced, through which the whole process can be simplified by skipping a sweeping search of all receivers for every ray.

Table I. Data structure of window and door "Polygon".

Parameter Name	Remarks
Vertex	List of vertexes window or door
Glass_Vertex	List of vertexes window or door shroud (such as glass)
now_room	Index of room the window or door belong to
next_room	Index of Room the window or door connect with
Reflectance	Reflectance of shroud
Propagation	Transmission coefficient of shroud
ScatteringCoefficient	Scattering coefficient of shroud

Table II. Data structure of the surface "Plane". Note: a, b, c, d are four parameters of the plane equation: $ax + by + cz + d = 0$.

Parameter Name	Remarks
a	Parameter a in the plane equation
b	Parameter b in the plane equation
c	Parameter c in the plane equation
d	Parameter d in the plane equation
Reflectance	Reflectance of the surface
ScatteringCoefficient	Scattering coefficient of the surface
DW	List of windows and doors contained in the surface
outsideflag	Determine whether the surface is an exterior one
Vertex	List of vertexes on the surface (only exterior surface recorded)

Table III. Data structure of the room "Room".

Parameter Name	Remarks
List_plane	List of surfaces composed of the Room
Receivers	Receivers in the Room

The basic rules of space partitioning are as follows: (1) any Room indoor after space partitioning must be convex polyhedron, in order to ensure that the closest collision point is a valid intersection; (2) an outdoor space is defined as "Room 0" which can be concave, because it only be used before the rays go into the indoor space, but not relate to the ray tracing process indoor; (3) any door or window can only belong to one Room and connect with another one.

2.1.3. The data structure of space partitioning

Using the C# language, surfaces, windows and Rooms are defined as classes, their data structures are shown in Tables I, II, III respectively. Each Room consists of several surfaces with each surface containing several doors or windows. The Rooms are connected by doors or windows. The relation between each factor is shown in Figure 2.

2.1.4. The procedure of ray tracing after space partitioning

The procedure of ray tracing after space partitioning is shown in Figure 3. Supposing the sound source is a point

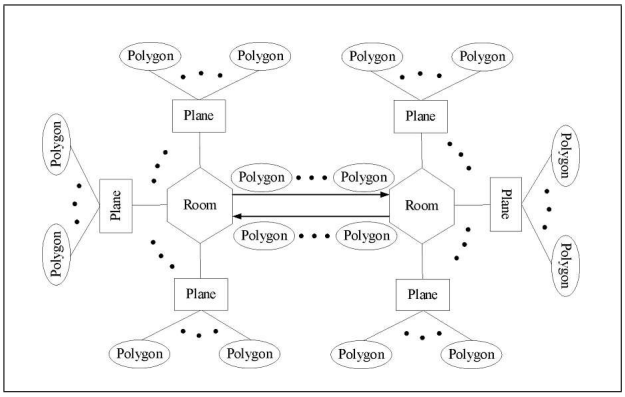

Figure 2. The relationship between each factor.

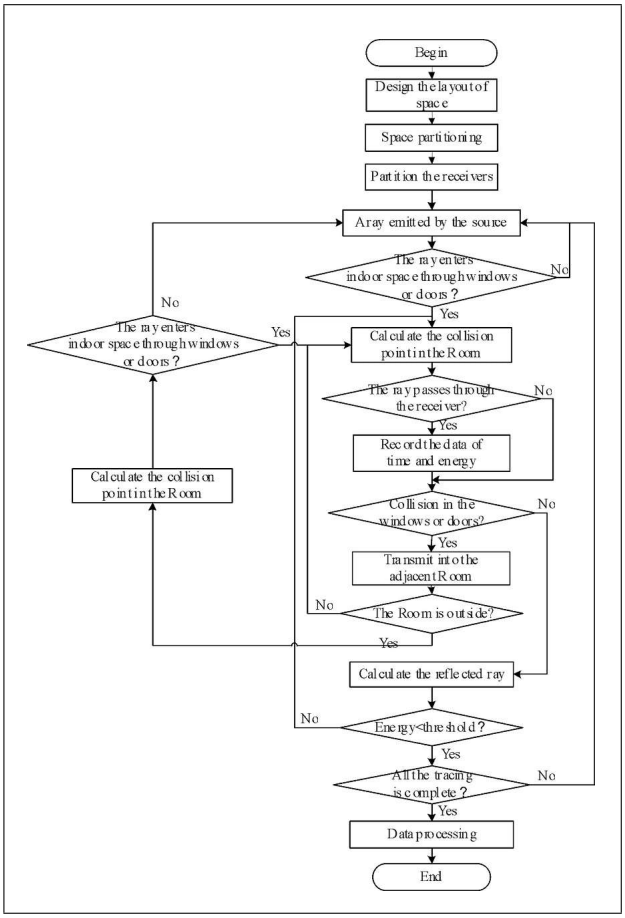

Figure 3. Process of the ray tracing.

source, and its energy is equally allocated to the rays sent out in all directions. In this case, if the sound power level of the source is L_{W0}, the sound power carried by each ray arrives at

$$I_0 = \frac{10^{(0.1L_{W0}-12)}}{n}, \tag{1}$$

where n is the total number of the rays. After the k-th reflection, the energy of each ray becomes

$$I_k = I_0\,\alpha^{k-1}, \tag{2}$$

in which α is the reflectance. When the ray tracing is finished, the receiver's sound pulses $I(t)$ varying with time can be seen. Then the receiver's SPL can be calculated by

$$\mathrm{SPL} = 120 + 10\log_{10}\left(\int_0^{\infty} I(t)\,\mathrm{d}t\right). \tag{3}$$

2.2. The simulative model of diffraction

Diffraction is a unique phenomenon of wave, which can not be directly simulated using the ray tracing method, so the simulation of sound diffraction should be completed separately. Considering both the complexity of diffraction path and the gradually diminishing contribution of diffraction as diffraction times increase, only the primary diffraction (Path ① in Figure 4) and the simple double diffraction along the surfaces (Path ② in Figure 4) will be included.

According to the "Norm on Acoustical Design and Measurement of Noise Barriers [37], the attenuation of diffraction is

$$\Delta L_d = \begin{cases} 20\lg\frac{\sqrt{2\pi N}}{\tanh\sqrt{2\pi n}} + 5, & N > 0, \\ 5, & N = 0, \end{cases} \tag{4}$$

where N is the Fresnel number, $N = 2(A+B-d)/\lambda$, λ is the wavelength of wave, in m. d represents the distance between source and receiver (m), A is the distance between source and the summit of acoustic barrier (m) and B is the distance between receiver and the summit of acoustic barrier (m). Note: the frequency of traffic noise is taken as 500 Hz [38, 39], so $\lambda = 340\,\mathrm{m/s} / 500\,\mathrm{Hz} = 0.68\,\mathrm{m}$. This equation applies only to simple double diffraction and to the receivers in the "geometric shadow" of the diffraction, since the "outside-shadow" diffractions contribute very little.

2.3. The dynamic simulation method of traffic noise spreading in indoor space

In an environment of urban roads mixed with buildings, traffic noise can penetrate a building through windows and doors, exerting an external influence on people indoors. Therefore, an effective method is needed to help reduce the impact of traffic noise. The dynamic simulation method of traffic noise spreading indoors can be accomplished by combination of microscopic traffic simulation, vehicle noise emission model and ray tracing method. The simulation process is illustrated in Figure 5. Firstly, road network was built in the Modeller of Paramics, a traffic microscopic simulation software. The properties of roads (the number of roads, the width of roads and the limited speed on the roads), the properties of vehicles (the types of vehicles, the proportion of different vehicles) and OD matrix (traffic volumes between different origin-destination pairs) can be set. At the same time, Application Procedural Interface (API) was programmed in the C++ language to acquire the location and speed of travelling vehicles. Even though these information obtained from Paramics may be a little different from the reality, this traffic micro-simulation model has been used in a number of studies in China and North America [40]. Secondly, the sound power level of vehicles L_{W0} was calculated based on the vehicle noise emission model. Thirdly, the rays which go through the windows are traced taking into consideration of diffraction. The whole process of traffic noise spreading indoors is thoroughly simulated, and thus the indoor sound field distribution and dynamical change of the indoor traffic noise could be obtained.

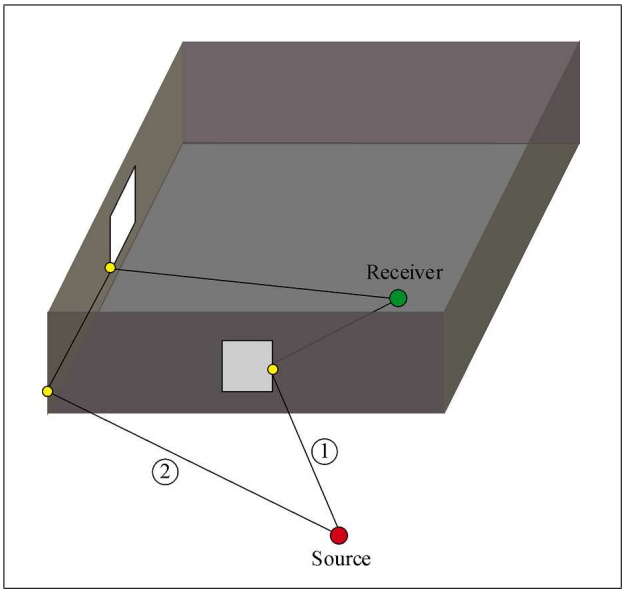

Figure 4. Schematic diagram of primary diffraction and simple secondary diffraction.

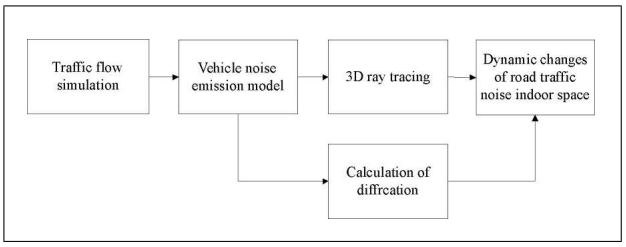

Figure 5. Process of traffic noise simulation in indoor space.

Through experiment, the relation between the vehicle speed and the sound pressure level L_0 of a single vehicle (including light, medium and heavy vehicle) in the 7.5 m reference distance [17] can be obtained by the formula

$$L_0 = \begin{cases} 24.92\log_{10}(v) + 27.96, & \text{Light vehicle,} \\ 36.73\log_{10}(v) + 16.44, & \text{Medium vehicle,} \\ 29.71\log_{10}(v) + 31.77, & \text{Heavy vehicle.} \end{cases} \tag{5}$$

The sound field in the experiment is hemisphere, thus the sound power of each type of vehicles is given by

$$W_0(v) = 2\pi\, 7.5^2\, 10^{0.1L_0(v)-12}. \tag{6}$$

Table IV. Statistical data of simulative results in example 1 (in dB).

	Room1	Room2	Room3
L_{eq}	65.2	54.8	64.2
L_{10}	67.0	56.7	66.0
L_{50}	63.6	52.8	62.3
L_{90}	58.3	48.5	56.4
L_{NP}	73.8	62.9	73.8

3. Examples and discussion

3.1. Example 1

3.2. Basic parameter

We adopt the proposed method to simulate the dynamic traffic noise in indoor space with the layout as shown in Figure 6. This layout is easy to be changed into different layouts, bringing convenience for demonstrating the different efficiency improvement of different layouts. To be simple but reasonable, suppose that the length of the two-lane two-way road is 500 m; the traffic flow is 3000 veh/h; the ratio of the light, medium and heavy vehicles is respectively 60%, 25% and 15%; the average speed is 50 km/h; the distance between the building and the street center line is 10 m. The height of the road is 0 m. The heights of the floor and the ceiling of the building are respectively 10 m and 14 m. The building is 20 m in both width and length, and its floor area is 400 m^2. The sizes of doors and windows are: 2 m×3 m and 2 m×2 m. Further, according to reality, the floor can be assumed to be concrete without cover, whose absorption coefficient is 0.05 [41]; the walls and ceiling can be suggested to be gypsum board with ½ in thickness, whose absorption coefficients are both 0.05 [42]. However, one study [21] pointed out that it is not possible to measure all of those coefficients, then their estimation becomes a guess. Therefore, to some extent, for the other coefficients we can make an ideal assumption that the reflecting, scattering and transmission coefficients of all these surfaces are respectively 0.9, 0.05 and 0. The radius and height of receivers are respectively 0.5 m and 11.5 m (1.5 m above the floor). The transmission coefficients of windows and doors open are all 1, while the reflecting and scattering coefficients are both 0. In this study, once sound is scattered upon reflection, that scattered sound is then ignored.

3.3. Simulative result

The distribution of simulation L_{eq} of indoor space is shown in Figure 7. It can be easily seen from Figure 7 that L_{eq} near windows is the highest, which can reach more than 70 dB. Because the floor of the building is 10 m high above the road, the distribution of the noise in the Room with the windows toward the road ("Room1" "Room3") takes a form of ribbon.

The statistical data of indoor noise in each Room is shown in Table IV. The average level of L_{eq} in the

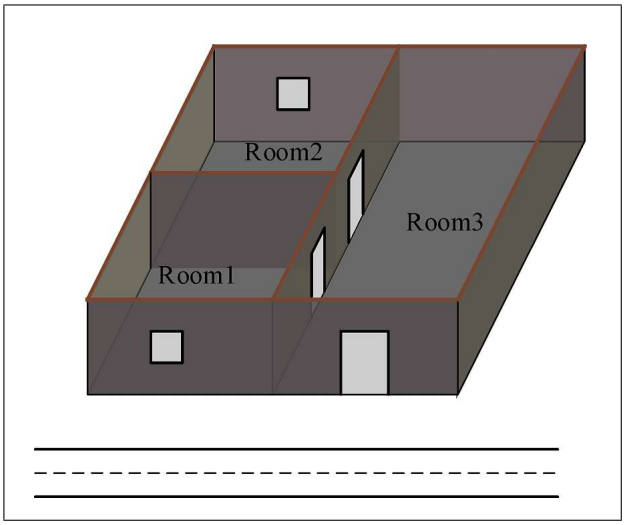

Figure 6. Indoor layout of example 1.

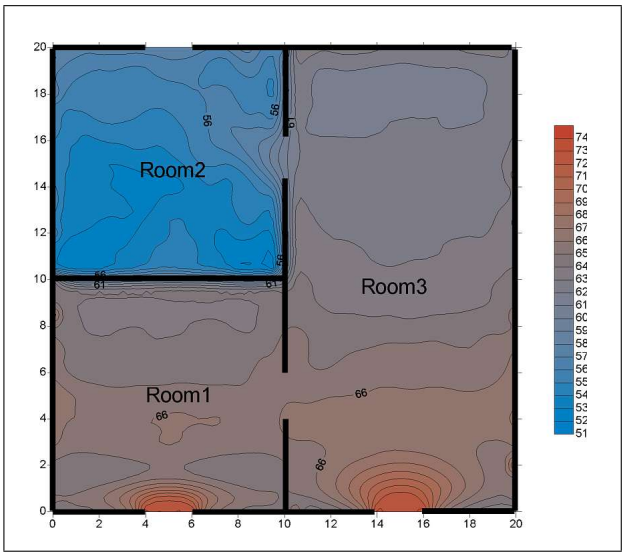

Figure 7. The distribution of indoor noise in example 1 (in dB).

Rooms with windows or doors toward the road ("Room1" "Room3") is proximately 10dB higher than that of the Room ("Room2" without windows or doors toward the road. Besides, the noise is relatively evenly distributed in each Room, and the average level difference between L_{10} and L_{90} is only 8–10dB.

3.3.1. Comparison with before space partitioning

Before space partitioning, all the surfaces are included in the process of calculating the intersection with the average search length ASL $= (n + 1)/2$, where n is the number of surfaces. After space partitioning, only the surfaces belonging to the Room where ray stays need to be traversed. So the average search length is ASL $= (s + 1)/2$, where s is the number of surfaces in each Room.

In this example, $n = 16$, $s = 6$, so the ratio of average search length before-and-after space partitioning is 17/7. And the actual calculation time is 590 minutes before space partitioning and 235 minutes after space partition-

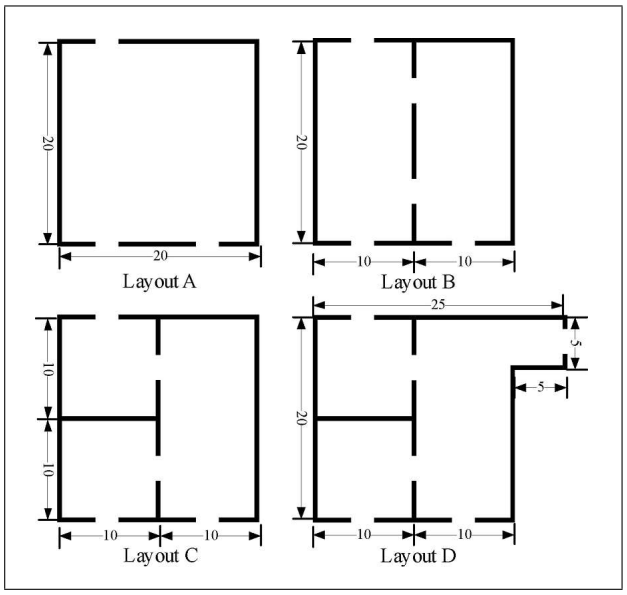

Figure 8. Four different layouts.

Table V. Optimization rate of different layouts. t_b: Computational time before space partitioning (min), t_a: Computational time after space partitioning (min).

Layout	t_b	t_a	Optimization rate
Layout A	538	471	12%
Layout B	553	276	50%
Layout C	590	235	59%
Layout D	1046	373	64%

Table VI. Statistical data of simulative results (L_{eq} in dB) with (Diff) and without (No diff) considering diffraction.

	Room1	Room2	Room3	Overall
Diff	65.2	54.8	64.2	62.1
No diff	63.8	54.0	63.4	61.2
Increment	1.4	0.8	0.8	0.9

ing. In other words, after space partitioning, the computational time reduces by 355 minutes and the optimization rate is 60%.

In addition, before space partitioning, the computational time increases as the number of indoor surfaces grows. But after space partitioning, it is determined by the number of surfaces in each Room, instead of being influenced by the total number of surfaces. As a result, the more complicated the indoor layout is, the larger the number of concave spaces is and the higher optimization rate will be after partitioning (see in Figure 8 and Table V).

3.3.2. Analysis of the influence of diffraction

By comparing the distributions of indoor noise before-and-after considering the influence of diffraction (see Figure 9 and Figure 7), the diffraction increment (see Figure 10) was obtained. The main resource of noise to the receivers closest to the window is the direct sound. That

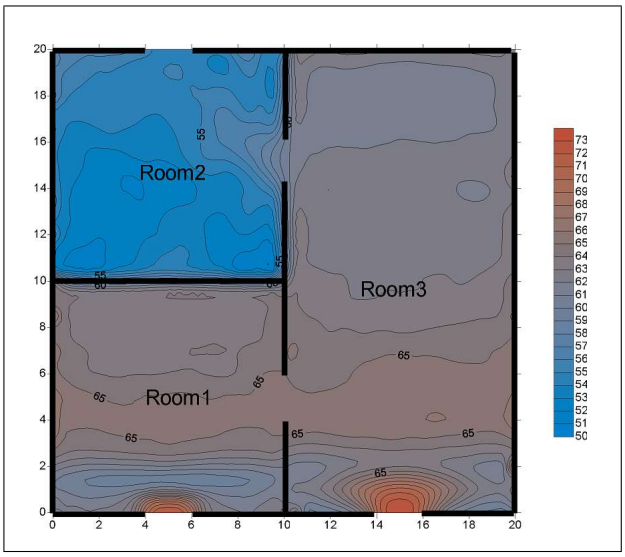

Figure 9. Distribution of indoor noise without considering the effect of diffraction (in dB).

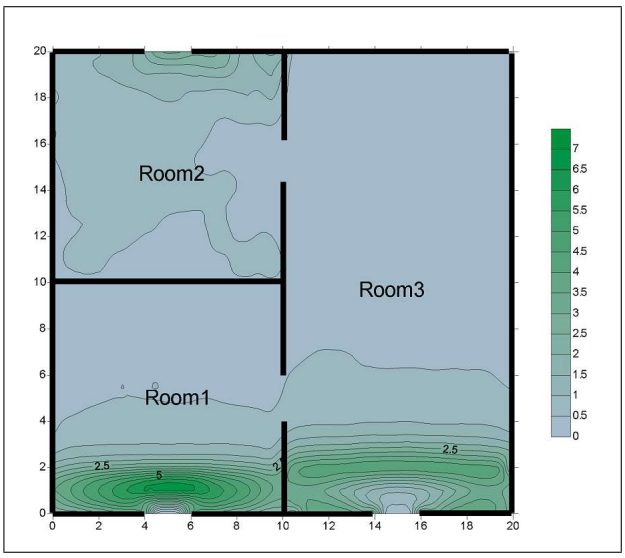

Figure 10. Increment of diffraction (in dB).

is to say, diffraction has little influence on it, whereas the receivers a little farther from the window suffer the most from the effect of diffraction as the rays can not reach there directly. The impact of diffraction on the receivers away from the windows gradually diminishes as the distance increases.

Table VI shows the statistical result of simulations. It can be concluded that diffraction has the most significant effect on "Room1", 1.4 dB, and 0.8 dB for both "Room2" and "Room3". The overall increment to the interior space is 0.9 dB. Although the influence is very small, the diffraction should be considered since it is a necessary part of simulation and its computation cost is only 11 minutes, far more less than that of the whole simulation, 471 minutes.

Table VII. Statistical results of simulation before and after the windows are closed (in dB).

	Balcony	Room1	Room2	Room3	Room4	Overall
before	72.8	61.3	66.2	66.2	68.6	63.3
after	72.8	61.3	54.4	54.6	57.4	58.1

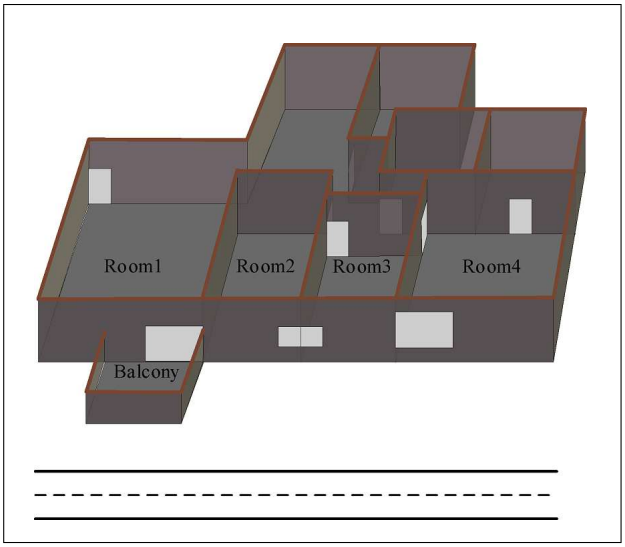

Figure 11. The indoor layout of example 2.

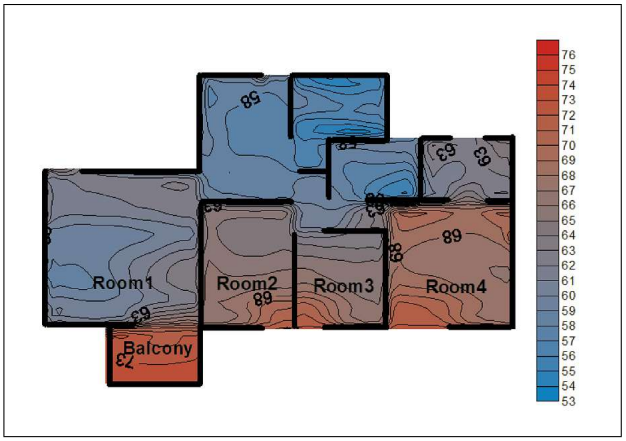

Figure 12. Distribution of indoor noise in example 2 (in dB).

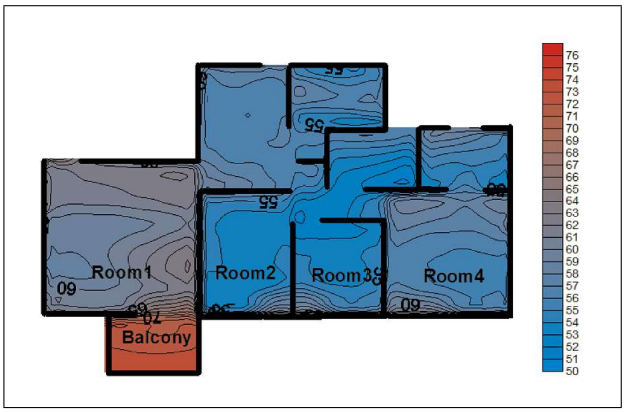

Figure 13. Distribution of indoor noise when the windows next to the road are closed (in dB).

3.4. Example 2

3.4.1. Basic parameter

The proposed method was applied in simulating the dynamic traffic noise for another indoor space as shown in Figure 11. It is a real layout located in Guangzhou city, and it is complex enough to point out the applicability of the method. Suppose that the length of the two-lane two-way road is 500 m; the traffic flow is 3000 veh/h; the percentages of the light, medium and heavy vehicles are respectively 60%, 25% and 15%; the average vehicle speed is 50 km/h; the distance between the building and the street center line is 10 m; the height of the road is 0 m. The heights of the floor and the ceiling of the building are respectively 10 m and 14 m. The height of balcony is 1 m. The building is 15 m in length and 10 m in width, and its floor area is 103 m^2. The sizes of doors, small windows and big windows are: 2 m×3 m, 1 m×1 m and 2 m×2 m. Similar to example 1, the floor is concrete without cover, and the walls and ceiling gypsum board. Then their reflecting, scattering, absorption and transmission coefficients are respectively 0.9, 0.05, 0.05 and 0. The radius and height of receiving ball are respectively 0.5 m and 11.5 m (1.5 m above the floor). The transmission coefficients of windows and doors open are all 1, while the reflecting and scattering coefficients are both 0.

3.4.2. Simulative result

The distribution of indoor noise is shown in Figure 12. It can be easily noted that the Balcony and Rooms ("Room2", "Room3" and "Room4" next to the road are most heavily affected by traffic noise. The maximum L_{eq} is higher than 70 dB and the average value is over 66 dB (see Table VII). Due to the shielding effect of balcony, traffic noise has a smaller influence on "Room1" in which the average L_{eq} is only 61.3 dB (see Table VII).

3.4.3. The influence of windows on indoor noise

Figure 13 shows the distribution of simulation L_{eq} in the indoor space when the windows in each Room ("Room2", "Room3" and "Room4") next to the road are closed. In this study, the windows are suggested to be double glazing with 2–3 mm glass, whose absorption coefficient is 0.05 [41], and the other coefficients such as reflecting, scattering, and transmission are assumed to be 0.9, 0, and 0.05. It can be seen that the average of in "Room2" "Room3" and "Room4" reduces by 11.8 dB, 11.6 dB and 11.2 dB separately. The overall L_{eq} declines by 5.2 dB.

Table VIII. Statistical data of simulative results in different floors (in dB).

	Balcony	Room1	Room2	Room3	Room4	Overall
Floor1	75.5	63.8	69.1	69.4	70.8	65.5
Floor2	73.9	61.4	67.3	67.8	70.0	64.1
Floor3	72.8	61.3	66.2	66.2	68.6	63.3
Floor4	71.7	61.4	64.7	65.1	67.0	62.7
Floor5	70.8	61.2	63.6	63.5	65.8	61.9

3.4.4. Analysis of indoor traffic noise distribution on different floors

Table VIII indicates the statistical results obtained by simulation of several floors (from the 1st floor to the 5th). As is demonstrated in Table VIII and the line of "Overall" in Figure 14, the higher the altitude of the floor gets, the less the overall L_{eq} is. Rising from 1st floor to 2nd floor sees the most significant decline, which is 1.4 dB; besides, the decreasing extent from 2nd floor to 3th floor, from 3th floor to 4th floor, from 4th floor to 5th floor are 0.8 dB, 0.6 dB and 0.8 dB respectively.

The lines of "Balcony", "Room2", "Room3" and "Room4" in Figure 14 clearly show that the L_{eq} of indoor noise declines as the altitude of floor gets higher. However, the line of "Room1" only shows downslide between 1st floor and 2nd floor, with the rest almost remaining steady. In other words, the L_{eq} rarely changes as the altitude of floor increases. This phenomenon is mainly caused by the shielding effect of the balcony. On the first floor, lots of rays from the sources of traffic noise can pass through the balcony and get into "Room1". While on the second floor, most rays can not get into "Room1" because of the shielding effect of the balcony, thus a significantly lower decibel of noise. Similarly, most rays on higher floors also can not get into "Room1" because of the shielding effect of balcony, so the lines remain steady for the rest.

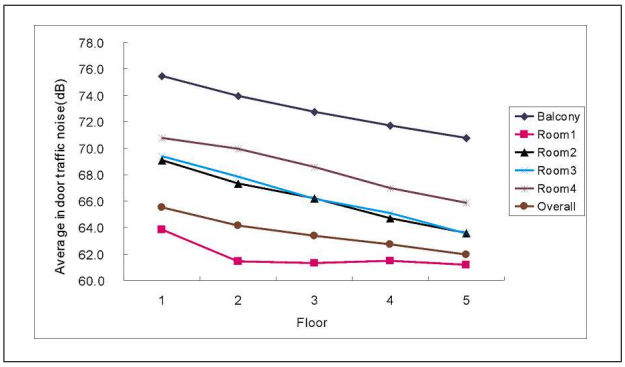

Figure 14. Average indoor traffic noise of different Room in different floors.

3.5. Analysis of indoor and outdoor traffic noise distribution

The distribution of indoor and outdoor traffic noise was illustrated in Figure 15. The parameters of the layout were the same with example 1 except that the sound source was only one car. As is demonstrated in Figure 15, the indoor traffic noise distribution renders the propagation of sound rays well. The outdoor traffic noise distribution clearly shows that the L_{eq} declines because of the shielding effect of the building and the longer distance between the receiver and the source. The noise distribution particularly near the window behind the building is higher, because these areas are affected by the sound rays which come out through the window.

The distribution of indoor and outdoor traffic noise in the layout (see Figure 11) before and after the windows in each Room ("Room2", "Room3" and "Room4") next to the road are closed was illustrated in Figure 16 and Figure 17 respectively. The parameters were the same with example 2. Table IX indicates the statistical results. It shows that when the windows near the road are open, the average

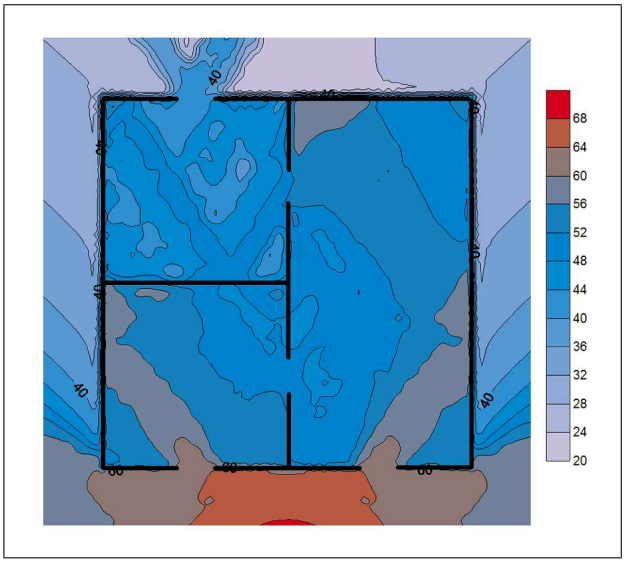

Figure 15. Distribution of indoor and outdoor traffic noise in example 1 (in dB).

Table IX. Statistical data of simulative results (in dB) before and after the windows are closed .

	Before	After
Average indoor traffic noise	63.3	58.1
Average outdoor traffic noise	70.8	70.9
Average outdoor traffic noise in front of the building	73.8	73.9
Average outdoor traffic noise behind the building	67.9	67.8

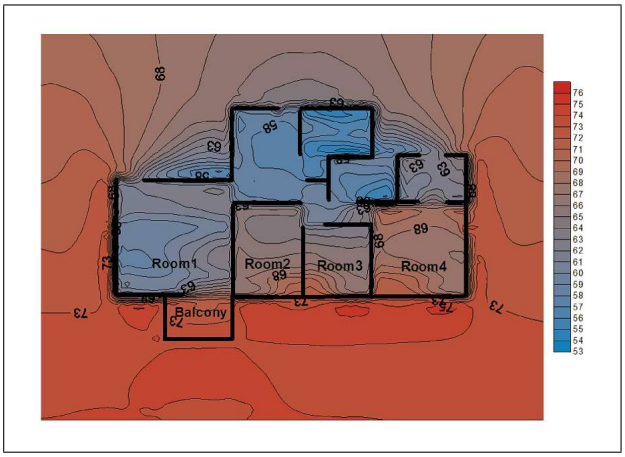

Figure 16. Distribution of indoor and outdoor traffic noise in example 2 when the windows near the road are open (in dB).

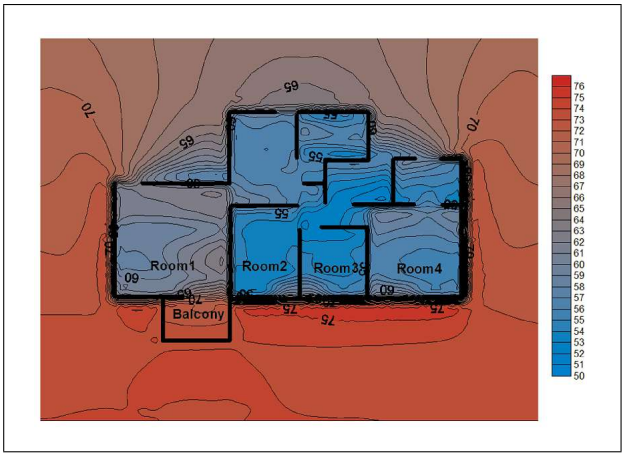

Figure 17. Distribution of indoor and outdoor traffic noise in example 2 when the windows near the road are closed (in dB).

indoor traffic noise is 7.5dB lower than the average outdoor noise. However, after these windows are closed, the level difference between average indoor and outdoor traffic noise becomes much bigger, 12.8 dB, reducing the average indoor traffic noise level by 5 dB, while the outdoor traffic noise nearly keeps the same. On the other hand, no matter whether the windows near the road are closed or not, the level difference between the average outdoor traffic noise in front of the building and the one behind the building is nearly the same, about 6 dB.

4. Conclusion

This study simplifies the calculation of the ray tracing through space partitioning. It also achieves the dynamic simulation of indoor traffic noise in the porous connected space in combination of microscopic traffic simulation, the vehicle noise emission model, ray tracing and by consideration of the influence of diffraction. Suitable for analysis of the impact of different building layouts and different floors on the indoor traffic noise distribution, and the comparison of indoor and outdoor traffic noise distribution, the proposed method has a wide application prospect.

The windows and floors of apartments have a significant influence on indoor traffic noise. Simulative results show that the decibel of indoor traffic noise next to roads decreases by approximately 11 dB with the windows closed. The results also indicate that the decibel of indoor noise decreases as the floor gets higher, especially for the apartments whose windows face the road and the balcony, where the noise declines by 1–2 dB and 0.9–1.6 dB respectively as the floor climbs up. However, compared with the other Rooms, the L_{eq} of "Room1" rarely changes from 2nd to 5th floor. The reason might be that, from 2nd floor most rays couldn't transmit into "Room1" because of the shielding effect of the balcony. From this point, a balcony can help to reduce the noise pollution, especially for lower floor. Further, the level difference between average indoor and outdoor traffic noise is 7.5 dB and 12.8 dB respectively before and after the windows are closed. And the average outdoor traffic noise in front of the building is about 6dB higher than the one behind the building. Besides, the noise distribution near the window behind the building is found to be much higher than around areas due to the affection of the sound rays from indoor space. Another interesting finding is that the average noise level of the outdoor traffic noise in front of the building is always 6dB higher than the one behind the building regardless of the status of windows face to the road.

However, there are two main limitations of this work. First of all, the accuracy of the simulation method used for traffic noise from outdoor to indoor space should be verified based on the real measurement data. Secondly, different coefficients of the materials should be more realistic but not only be ideally assumed. Thus, the experiments monitoring indoor and outdoor sound fields of different floors need to be taken in the future, and the coefficients of materials should be collected by doing experiments.

Acknowledgement

This work was supported by the National Natural Science Foundation of China (51178476).

References

[1] H. Doygun, D. G. Kusat: Analysing and mapping spatial and temporal dynamics of urban traffic noise pollution: a case study in Kahramanmaras, Turkey. Environ. Monit. Assess. **142** (2008) 65–72.

[2] R. Klaboe, E. Engelien, M. Steinnes: Context sensitive noise impact mapping. Appl. Acoust. **67** (2006) 620–642.

[3] K. Kaliski, E. Duncan, J. Cowan: Community and regional noise mapping in the United States. Sound. Vibr. **41** (2007) 14–19.

[4] L. Chi-wing, L. Chee-kwan, L. A. Shiu-wai, Y. M. Kwok-leung, L. Kin-che: Advancement of three-dimensional noise mapping in hong kong. Appl. Acoust. **72** (2011) 534–543.

[5] P. Pamanikabud, M. Tansatcha: Geoinformatic prediction of motorway noise on buildings in 3D GIS. Transp. Res. Part D: Trans. Environ. **14** (2009) 367–372.

[6] P. Pamanikabud, M. Tansatcha: 3D analysis and investigation of traffic noise impact from a new motorway on building and surrounding area. Appl. Acoust. **71** (2010) 1185–1193.

[7] C. Mak, W. Leung, G. Jiang: Measurement and prediction of road traffic noise at different building floor levels in Hong Kong. Build. Serv. Eng. Res. Technol. **31** (2010) 131–139.

[8] P. Lee, Y. Kim, J. Jeon, K. Song: Effects of apartment building facade and balcony design on the reduction of exterior noise. Build. Environ. **42** (2007) 3517–3528.

[9] S. K. Tang: Noise screening effects of balconies on a building façade. J. Acoust. Soc. Amer. **118** (2005) 213–221.

[10] C. Buratti: Indoor noise reduction index with open window. Appl. Acoust. **63** (2002) 431–451.

[11] F. Marian: Interaction of environmental noise and building construction. Cesb 10. Cent. Eur. Sustainable. Build. -From Theory To Pract. (2010) 467–470.

[12] L. Feng, C. Ming, L. Jike: Intersection traffic noise simulation method based on microscopic traffic simulation. Environ. Sci. Technol. **33** (2010) 179–182.

[13] R. R. K. Jones, D. C. Hothersall, R. J. Salter: Techniques for the investigation of road traffic noise in regions of restricted flow by the use of digital computer simulation methods. J. Sound Vibr. **75** (1981) 307–322.

[14] Y. Oshino, K. Tsukui, H. Tachibana: Road traffic noise prediction taking account of transient vehicle running condition. Inter-noise, Liverpool, UK, 1996, 3117–3120.

[15] C. Ming, L. Feng, L. Jike: Dynamic simulation and characteristics analysis of traffic noise at signal-controlled pedestrian crossing junction. Noise. Control. Eng. J. **59** (2011) 549–555.

[16] K. Tsukui, Y. Oshino, G. V. Blokland, H. Tachibana: Study of the road traffic noise prediction method applicable to low-noise road surfaces. Acoust. Sci. Technol. **31** (2010) 102–112.

[17] L. Feng, C. Ming, L. Jike, Y. Zhi: Dynamic traffic noise simulation at a signalized intersection among buildings. Noise. Control. Eng. J. **59** (2011) 202–210.

[18] L. Leclercq, E. Chevallier, A. Can, M. Nadji: Improving noise assessment at intersections by modeling traffic dynamics. Transp. Res. Part D: Trans. Environ. **14** (2009) 100–110.

[19] T. Suzuki, K. Tsukui, Y. Oshino, H. Tachibana: Road traffic noise prediction model around signalized intersections. Inter-Noise, Seogwipo, Korea, 2003, 1870–1873.

[20] L. Ledercq, E. Chevallier, J. Lelong, R. Chatagnon: Dynamic noise modeling at roundabouts. Appl. Acoust. **70** (2009) 761–770.

[21] O. E. David: Room acoustics modeling using the ray-tracing method: Implementation and evaluation. Licentiate Thesis. University of Turku, Department of Physics, 2005.

[22] A. M. Ondet, J. L. Barbry: Modeling of sound propagation in fitted workshops using ray-tracing. J. Acoust. Soc. Am. **85** (1989) 787–796.

[23] J. J. Embrechts: Broad spectrum diffusion model for room acoustics ray-tracing algorithms. J. Acoust. Soc. Am. **107** (2000) 2068–2081.

[24] A. Pompei, M. A. Sumbatyan, N. F. Todorov: Computer models in room acoustics: The ray tracing method and the auralization algorithms. Acoust. Phys. **55** (2009) 821–831.

[25] A. Krokstad, S. Strom, S. Sarsdal: Calculating the acoustical room response by the use of a ray tracing technique. J. Sound. Vibr. **8** (1968) 118–125.

[26] A. Kulowski: Algorithmic representation of the ray tracing technique. Appl. Acoust. **18** (1985) 449–469.

[27] L. Nijs, G. Jansens, G. Vermeir, M. van der Voorden: Absorbing surfaces in ray-tracing programs for coupled spaces. Appl. Acoust. **63** (2002) 611–626.

[28] L. N. Yang, B. M. Shield: Development of a ray tracing computer model for the prediction of the sound field in long enclosures. J. Sound. Vibr. **229** (2000) 133–146.

[29] M. Hodgson, G. Wong: Ray-tracing prediction of optimal conditions for speech in realistic classrooms. Appl. Acoust. **70** (2009) 915–920.

[30] Z. Congzhe, Z. Yue: A generalized ray-tracing algorithm for integrated visual and auditory rendering in room acoustics. Civ. Eng. Environ. Syst. **18** (2001) 19–34.

[31] M. Hodgson: Ray-tracing evaluation of empirical models for predicting noise in industrial workshops. Appl. Acoust. **64** (2003) 1033–1048.

[32] J. Keranen, E. Airo, P. Olkinuora: Validity of ray-tracing method for the application of noise control in workplaces. Acta Acustica united with Acustica **89** (2003) 863–874.

[33] J. Zhong-Jin, C. Tie-Jun: Spatial distribution prediction of steady-state sound field with the ray-tracing method. J. Vibr. Acoust. **130** (2008) 064503.

[34] F. R. Feito, J. C. Torres: Inclusion test for general polyhedra. Comput. Graph. **21** (1997) 23–30.

[35] Y. E. Kalay: Determining the spatial containment of a point in general polyhedra. Comput. Graph. Image. Process. **19** (1982) 303–334.

[36] A. Kulowski: Optimization of a point-in-polygon algorithm for computer models of sound field in rooms. Appl. Acoust. **35** (1992) 63–74.

[37] HJ/T 90-2004: Norm on acoustical design and measurement of noise barriers (in Chinese). Ministry of Environmental Protection, Beijing, 2004.

[38] C. M. Harris: Handbook of noise control. Hill Book Co., N.Y., 1979. 3-1-16.

[39] T. M. Barry, J. A. Reagan: FHWA high way traffic noise prediction model. FHWA-RD-77-108. Washington DC: U. S. Department of Transportation, 1978.

[40] T. Oketch, M. Carrick: Calibration and validation of a micro-simulation model in network analysis. Proceddings of 84th TRB Annual Meeting, Washington, DC, 2005.

[41] M. Vorländer: Auralization: Fundamentals of acoustics, modelling, simulation, algorithms and acoustic virtual reality. Springer, 2008.

[42] M. D. Egan: Architectural acoustics. J. Ross Publishing, 2007.